Mitochondrion 85 (2025) 102080

Contents lists available at ScienceDirect

Mitochondrion

journal homepage: www.elsevier.com/locate/mito

The homoplasmic *MT-TK* m.8357T > C mtDNA variant as a cause of multiorgan mitochondrial disease

Luisa Zupin [a,1,*], Valeria Capaci [a,1], Maria Teresa Bonati [a], Eleonora Lamantea [b], Muhammad Suleman [c], Andrea Marsala [b], Fulvio Celsi [a], Beatrice Spedicati [a,d], Sergio Crovella [e], Giulia Gortani [a], Giorgia Girotto [a,d], Irene Bruno [a], Massimo Zeviani [a,f,*]

[a] Institute for Maternal and Child Health IRCCS Burlo Garofolo, 34137 Trieste, Italy
[b] Unit of Medical Genetics and Neurogenetics, Fondazione IRCCS Istituto Neurologico Carlo Besta, 20126 Milan, Italy
[c] Centre for Biotechnology and Microbiology, University of Swat, 19130 Swat, Pakistan
[d] Department of Medicine, Surgery and Health Sciences, University of Trieste, 34149 Trieste, Italy
[e] Department of Genetics, Federal University of Pernambuco, 50670-901 Recife, Brazil
[f] University of Padova Department of Neuroscience, Veneto Institute of Molecular Medicine, Via Orus 2, Padova 35128, Italy

ARTICLE INFO

Keywords:
Mitochondrial disease
Heteroplasmy
mt-tRNA-Lys

ABSTRACT

The diagnosis of disorders associated with mitochondrial DNA (mtDNA) variants presents substantial complexity due to their genetic and clinical heterogeneity, which is largely influenced by mtDNA heteroplasmy. However, the level of heteroplasmy alone is often not sufficient to predict the clinical phenotype including its severity and progression.

This study concerns the characterization of the m.8357T > C variant in the *MT-TK* gene, encoding for mt-tRNA-Lys found in two pediatric siblings. Both had symptoms suggestive of a mitochondrial disease, including severe hearing loss, easy fatigability, decreased activity of mitochondrial complex I in muscle samples, epilepsy, metabolic acidosis with hyperkalemia, and mild kidney impairment.

The m.8357T > C mtDNA variant was homoplasmic in muscle, blood, urine and fibroblasts. Immortalized fibroblasts from the patients showed reduced activity of mitochondrial complexes I, III and IV, decreased mitochondrial respiration, and abnormal depolarization of the mitochondrial membrane potential. The mt-tRNA-Lys levels were reduced as compared to the mt-tRNA-Leu (UUR) or the snRNA encoded by *RNU6B* nuclear gene; the level of three mitochondrial DNA encoded proteins was decreased, altogether suggesting a defective translation machinery in cells carrying the variant. Consistently, fibroblasts from the mother, who had only mild hearing loss, despite high level of heteroplasmy, showed some biochemical abnormalities, however milder than in her daughter and son. Contrariwise, their maternal aunt, who showed intellectual disability, mild hearing loss, easy fatigability and weakness was also virtually homoplasmic for the m.8357T > C in blood and urinary sediment cells. These findings suggest the pathogenicity of the m.8357T > C variant but only in condition of homoplasmy.

1. Introduction

MtDNA is a circular double-strand molecule of 16569 bp, encoding 13 proteins involved in the formation of four out of the five canonical mitochondrial respiratory complexes: 7 subunits of complex I (cI), 1 of complex III (cIII), 3 of complex IV (cIV), 2 of complex V (cV), whereas complex II (cII) lacks any mtDNA-encoded protein subunit. Additionally, mtDNA encodes 22 tRNAs and two rRNAs, i.e., the entire RNA apparatus needed for *in situ* translation of the 13 protein-encoding genes (Ojala et al., 1981; Suzuki et al., 2011). The other proteins required for mitochondrial translation are encoded by nuclear DNA and imported from the cytoplasm (Fernandez-Vizarra and Zeviani, 2021). The mitochondrial genetic code differs from the universal nuclear genetic code, therefore *in situ* autonomous mitochondrial translation is essential for

* Corresponding authors at: Institute for Maternal and Child Health IRCCS Burlo Garofolo, Via dell'Istria, 65, 34137 Trieste, Italy.
E-mail addresses: luisa.zupin@burlo.trieste.it (L. Zupin), massimo.zeviani@burlo.trieste.it (M. Zeviani).
[1] These two authors contributed equally.

https://doi.org/10.1016/j.mito.2025.102080
Received 16 April 2025; Received in revised form 16 August 2025; Accepted 17 August 2025
Available online 18 August 2025
1567-7249/© 2025 The Authors. Published by Elsevier B.V. This is an open access article under the CC BY-NC-ND license (http://creativecommons.org/licenses/by-nc-nd/4.0/).

the production of mtDNA encoded proteins. The 22 mt-tRNAs are the minimal set required for mtDNA translation. However, two tRNAs are present for Leucine and two for Serine (Suzuki et al., 2020) while the only tRNA that is identical in both mitochondria and cytoplasm is tRNA for Lysine, however, the cytoplasmatic one is not imported into mitochondria (Suzuki et al., 2020, 2011).

About half of the mitochondrial diseases (MDs) caused by mitochondrial DNA (mtDNA) variations result from alterations in genes encoding one of the 22 mitochondrial transfer RNAs (mt-tRNA) (Abbott et al., 2014).

The phenotypic spectrum associated with the mt-tRNA gene variants is very broad, due, at least in part, to differences in heteroplasmy levels across tissues and the possible influence of nuclear-encoded modifiers. Generally, impaired mitochondrial protein biosynthesis leads to reduced mitochondrial respiratory activity, decreased oxygen consumption, and increased reliance on glycolysis resulting in elevated lactate levels (Jacobs, 2003).

Most frequent neurological MDs, such as Mitochondrial Encephalomyopathy, Lactic Acidosis and Stroke-like episodes (MELAS) and Myoclonic Epilepsy and Ragged Red Fibers (MERRF), are commonly associated with genetic variants in *MT-TL1* (m.3243A > G), and *MT-TK* (m.8344A > G) genes respectively. MELAS is characterized by stroke-like episodes, particularly the occipital and temporoparietal regions of the brain, associated with symptoms such as dementia, epilepsy, and spastic paralysis (El-Hattab et al., 2015). MERRF includes epileptic myoclonus, ataxia, dementia and, often, lipomas along the midline of the body (Velez-Bartolomei et al., 1993). However, clinical heterogeneity, even among individuals carrying the same genetic variant, and overlapping phenotypic features in different MDs, can further complicate the diagnosis. Variability in heteroplasmy levels across different tissues crucially contributes to the variability in disease presentation (Richter et al., 2021).

This study aimed to functionally characterize the mitochondrial DNA variant m.8357T > C in the *MT-TK*, gene encoding for mt-tRNA-Lys, identified in a single family along the maternal lineage. This variant was previously associated with familial multiple symmetric lipomatosis in a heteroplasmic condition with a lower mutational load (López-Gallardo et al., 2020).

2. Materials and methods

2.1. Subjects and primary cell line generation

Two siblings, 10 and 7 years old at the last follow-up, presenting symptoms suggestive of a mitochondrial disorder, were enrolled at the Institute for Maternal and Child Health IRCCS 'Burlo Garofolo', Trieste, together with their parents and relatives from the maternal lineage (aunt, uncle, and grandmother). The pedigree is shown in Fig. 1A. Each enrolled family member underwent a deep phenotyping as well as blood and urine sample collection for genetic analyses, moreover, muscle biopsies had been performed in the two siblings.

Punch skin biopsies were also collected from the siblings and their mother and primary fibroblast cell cultures were established. Finally, the fibroblasts were immortalized by using Lenti-hTERT-2A-CDK4 Virus, High Titer (LV677, ABM Applied Biological Materials, Canada).

Written informed consents for genetic tests and research were obtained from the parents of the siblings and from each enrolled family member.

2.2. Genetic analysis

DNA was extracted from blood samples using the QIAsymphony® DNA Midi on the QIAsymphony® SP platform (Qiagen, Hilden, Germany) following the manufacturer's instructions.

Whole Genome Sequencing (WGS) was performed on III-1 subject and his parents on an Illumina NovaSeq platform (Illumina Inc., San-Diego, CA, USA), by using TruGenome Undiagnosed Disease Test assessed in February 2019. Data generated at ≥ 30 fold coverage were aligned to Human Reference Genome (build at GRCh37.1). Both Single Nucleotide Variants (SNVs) and copy number variants (CNVs) were detected, while mitochondrial SNV > 3 % were interpreted for pathogenicity. Clinical report was generated by Illumina Clinical Services Laboratory.

Whole exome sequencing (WES) was performed in I-2, II-1, II-2, II-3, III-1 and III-2 (Fig. 1A) on an Illumina NextSeq 550 instrument (Illumina Inc., San Diego, CA, USA) by using the Twist Exome 2.0 plus Comprehensive Exome Spike-in kit (TwistBioscience, South San Francisco, CA, USA). The FASTQ files were analyzed by the enGenome s.r.l. pipeline (https://www.engenome.com/) for the identification of germline genetic variants. A VCF (variant calling format) file was generated for each individual and was analyzed through the enGenome Expert Variant

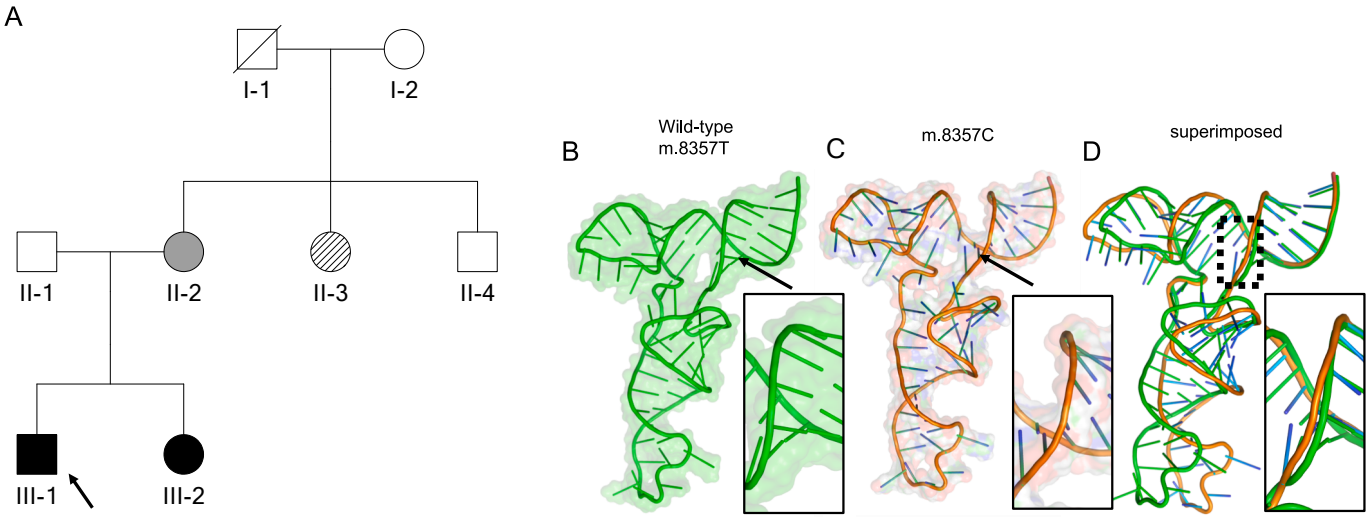

Fig. 1. A) the family pedigree: open symbols, unaffected; dark filled symbols, affected by more severe phenotype; grey symbol, affected by bilateral sensorineural hearing impairment; diagonal bar filled symbol, affected by a milder phenotype; arrow, proband, B) wild-type 3D tRNA conformation, C) mutated 3D tRNA conformation, D) superimposition of wild-type over mutant tRNA structure.

Interpreter (eVai) software (https://evai.engenome.com/).

Variants from WGS and WES were filtered based on the following criteria: 1) minor allele frequency (MAF) cutoff of 0.001; 2) pathogenicity, evaluated through several *in silico* prediction tools, including PolyPhen-2 (Adzhubei et al., 2013), Sorting Intolerant From Tolerant (SIFT), Pseudo Amino Acid Protein Intolerance Variant Predictor (PaPI score), Deep Neural Network Variant Predictor (DANN score), and dbscSNV score; 3) SNVs leading to synonymous amino acid substitutions not predicted as damaging, nor affecting splicing, or highly conserved residues were excluded; 4) quality score (QUAL cut off was set at < 20); 5) patients' phenotype and specific symptoms according to human phenotype ontology (HPO). The ClinVar (https://www.ncbi.nlm.nih.gov/clinvar/), the Human Gene Mutation Database (HGMD) professional (Qiagen), Online Mendelian Inheritance in Man (OMIM) (https://www.omim.org/), and DECIPHER (https://www.deciphergenomics.org) were used for the interpretation of selected variants. Variant classification was carried out following the American College of Medical Genetics and Genomics (ACMG) and Association for Molecular Pathology (AMP) criteria (McCormick et al., 2020; Richards et al., 2015).

For targeted mtDNA sequence, amplicons from PCR spanning entire mtDNA were diluted to a final concentration of 0.2 ng/mL, processed according to the Nextera XT DNA Library Prep protocol (Illumina, San Diego, CA) and sequenced afterwards by MiSeq Illumina as described in Legati et al. (Legati et al., 2021). For haplotypes and heteroplasmy analysis, reads generated were mapped to the Revised Cambridge Reference Sequence (NC_012920.1) using the dedicated application on BaseSpace website (Illumina, San Diego, CA) called mtDNA Variant Processor. The aligned reads were analyzed for variant calling and heteroplasmy level detection with mtDNA Variant Analyzer tool (Illumina, San Diego, CA).

Confirmation and segregation analyses of mtDNA variants were performed by Sanger sequencing.

2.3. Quantification of heteroplasmy

To quantify the variant m.8357T > C in muscle of two children the already reported Nextera XT strategy (Legati et al., 2021) on PCR fragment from m.8186 to m.8440 was used.

Additionally, DNA was extracted from blood and urine samples by using the Puregene Blood Kit (Qiagen) and with Quick-DNA Urine Kit (Zymo Research).

Heteroplasmy in all other tissues was assessed by PCR with primers specific to NGS (next generation sequencing) (5′- ACACTCTTTCCCTACACGACGCTCTTCCGATCT −forward primer target sequence-3′, 5′-GACTGGAGTTCAGACGTGTGCTCTTCCGATCT −reverse primer target sequence-3′), and Q5® High-Fidelity DNA Polymerase (NEB). The PCR products were purified with QIAquick PCR & Gel Cleanup Kit (Qiagen) and then sequenced on the MiSeq Illumina platform (Illumina). Custom pipeline was used to align the sequence on the mt-DNA references in IGV for heteroplasmy assessment.

2.4. Assessment of mtDNA copy number

The mtDNA Copy Number (CN) was measured through semi-quantitative Real Time PCR. The Taqman assays (Thermo Fisher Scientific) *MT-ND1*, (Hs02596873_s1, VIC) and *MT-ND3* (Hs02596875_s1 VIC) were used to evaluate mtDNA copy number, while the genomic noncoding RNA, *RPPH1* (Assay ID Hs03297761_s1 FAM) was employed as internal control (copy number equal to 2) in each reaction. TAQPATH PROAMP master mix (A30866) was used in a final volume of 20 μL with 20 ng of DNA on the CFX Opus instrument (Bio-rad, USA).

2.5. Biochemical enzymatic analysis of respiratory chain complexes

Biochemical activities of mitochondrial complexes were performed on muscle samples of the two siblings. The same activities were assessed in fibroblasts as well.

The muscle samples were homogenized mechanically, and the assay was performed on supernatant obtained after 800 xg centrifugation, while fibroblasts were harvested and permeabilized by digitonin treatment.

Biochemical analysis on muscle homogenates was performed as previously described (Bugiani et al., 2004) with some modification detailed in Bergonzini et al. (Bergonzini et al., 2025). Briefly, each mitochondrial complex activity was measured spectrophotometrically in a 500 μl reaction volume and the reactions were measured in duplicates using two different amounts of proteins and followed for 2 min at controlled temperature. The enzymatic activity for each complex was determined as nmol min-1 mg-1 of protein and normalized for citrate synthase (CS) activity.

Complexes I (NADH dehydrogenase), III (decylbenzylquinonol: cytochrome *c* oxidoreductase) and IV (Cytochrome *c* Oxidase) activities were measured in fibroblasts over time as previously described (Grazina, 2012) at the Biotek Cytation 5 cell imaging multimode reader (Agilent Technologies, USA). All the reagents employed in the assays were purchased from Sigma-Aldrich (Merck).

2.6. Oxygen consumption measurement

Oxygen consumption measurement was performed in fibroblasts by using the Oroboros High resolution respirometry (Oroboros Instrument, Austria).

Two million fibroblasts were resuspended in Mir05 medium (Oroboros instrument) and analysed with Oroboros by using SUIT-007 O2 pce D030 protocol. Standard respiration was analyzed, then, cells were digitonin-permeabilized, and consecutively treated with glutamate (leak respiration), ADP and malate (oxidative phosphorylation OXPHOS capacity), mitochondrial uncoupler carbonyl cyanide 3-chlorophenylhydrazone (CCCP) (electron transfer ET capacity) and antimycin A (residual oxygen consumption). The traces representing oxygen consumption were compared between controls and patients' fibroblasts.

2.7. RNA extraction and quantitative real-time PCR

500,000 cells were seeded on 60 mm plate, after 48 h they were harvested in TriFast (Euroclone, Italy) for total RNA extraction.

1.5 μg of high-quality total RNA (having A260:A230 ratio greater than 1.8; A260:A280 ratio between 1.9 and 2.0; and total RNA concentration greater than 100 ng/μl) was retrotranscribed using the rtStar™ tRNA Pretreatment & First-Strand cDNA Synthesis Kit (Cat# AS-FS-004, Arraystar, MD, USA). This kit consists of (i) a RNA demethylation reaction; immediately followed by (ii) phenol:chloroform RNA purification and then (iii) first strand cDNA synthesis has been performed as indicated by manufacturer. During retrotranscription,1 μl of RNA Spike-In was added to perform the cDNA quality control by qRT-PCR. The obtained cDNA was diluted 1:40 as suggested by the manufacturer protocol. Then qRT-PCR analyses were carried out on cDNAs retrotranscribed using the Arraystar SYBR® Green qPCR Master Mix (ROX +) (AS-MR-006-5, Arraystar) on the Real-Time CFX Opus platform (Bio-Rad). The quantification was based on the $2^{-\Delta\Delta Ct}$ method using the housekeeping control genes *RNU6B* and the mt-tRNA-Leu (UUR) as normalization reference.

Experiments were performed four times, and each sample was the average of a technical duplicate.

2.8. Western blot of the mtDNA encoded proteins

About 0,5 million fibroblasts were harvested and lysed in RIPA buffer (89900, Thermo Fisher Scientific, USA) plus Halt proteinase and phosphatase inhibitor, supplemented with Protease and Phosphatase Inhibitor Cocktail (Thermo Fisher Scientific). Bradford assay was used to

Table 1
Summary of the clinical findings of the patients and their family members, and HPO used in the genetic analyses. Age at last follow-up is reported next to each family member's pedigree ID.

III-1 (10 years)	III-2 (7 years)	II-3 (24 years)
- Facial dysmorphisms (Hypertelorism HP:0000316, Bulbous nose HP:0000414, Pointed chin HP:0000307)	- Facial dysmorphisms (Hypertelorism HP:0000316)	- Clumsiness HP:0002312
- Intellectual disability, mild HP:0001256	- Intrauterine growth restriction HP:0001511	- Intellectual disability, mild HP:0001256
- Delayed speech and language development HP:0000750	- Oligohydramnios HP:0001562	- Exercise-induced muscle fatigue HP:0009020
- Clumsiness HP:0002312	- Failure to thrive HP:0001508	- Action tremor HP:0002345
- Exercise-induced muscle fatigue HP:0009020	- Delayed speech and language development HP:0000750	- Anxiety HP:0000739
- EEG abnormality HP:0002353	- Absence seizure with eyelid myoclonus HP:0011149	- Mild neurosensory hearing impairment HP:0008587
- Progressive sensorineural hearing impairment HP:0000408	- Moderate sensorineural hearing impairment HP:0008504	
- Lactic acidosis HP:0003128	- Lactic acidosis HP:0003128	
- Metabolic acidosis HP:0001942	- Metabolic acidosis HP:0001942	
- Hyperkalemia HP:0002153	- Hyperkalemia HP:0002153	
- Hepatic steatosis HP:0001397	- Anemia of inadequate production HP:0010972	
- Anemia of inadequate production HP:0010972	- Bone marrow hypocellularity HP:0005528	
- Bone marrow hypocellularity HP:0005528	- Decreased activity of mitochondrial complex I HP:0011923	
- Decreased activity of mitochondrial complex I HP:0011923		
II-2 (32 years)	I-2 (53 years)	
- Mild neurosensory hearing impairment HP:0008587	- Frequent labyrinthitis episodes	

Table 2
Percentage of the heteroplasmy levels of m.8357T > C in different tissues of the family members.

	III-1	III-2	II-2	I-2	II-3	II-4
Percentage m.8357C						
Muscle	100 %	100 %				
Blood	100 %	100 %	84 %	56 %	96 %	36 %
Urine	99 %	99 %	94 %	78 %	99 %	40 %
Primary fibroblasts	98 %	99 %	81 %			
Immortalized fibroblasts	98 %	98 %	97 %			

quantify the lysates (Bio-Rad, #500-0006). Lysates were resolved by SDS/PAGE (Thermo Fisher Scientific) and incubated with antibodies anti cytochrome *b* (69202S, Cell Signalling Technology), anti cytochrome *c* oxidase 1 (PA5-115081, Thermo Fisher Scientific) anti-NADH dehydrogenase subunit 1 (PA5-120599 Thermo Fisher Scientific), anti actin (8H10D10 Cell Signalling Technology, used for normalization), and then with HRP secondary antibodies. Images were acquired using Clarity Max Western ECL Substrate on the ChemiDoc MP Imaging System (Bio-Rad). Intensity of the bands was quantified using ImageJ software and expressed as the ratio of the proteins of interest on actin band intensity.

2.9. Mitochondrial membrane potential measurement

About 10.000 cells were seeded on the 96 multi well black plate (Primo, Euroclone), then after plating, JC-1 probe was used to assess the mitochondrial membrane potential (MMP) at staining condition 5 μM at 37 °C for 1 h (T3168, Thermo Fisher Scientific), at the Cytation 5 Cell Imaging Multi-Mode Reader (Biotek, Winooski, VT, USA).

The fluorescence intensity ratio red (590 nm) to green (525 nm) was used to analyze the data.

2.10. Modeling of wild-type and mutant RNA molecule

To examine the effects of variant on the tRNA molecular structure, we modeled both wild-type and mutant tRNA molecules and then superimposed them to identify structural differences. The 2D structure of the tRNA was modeled by submitting the sequences of both wild-type and mutant to the RNAfold web server (http://rna.tbi.univie.ac.at//cgi-bin/RNAWebSuite/RNAfold.cgi/. Their 3D structures were generated using the RNAComposer web server (https://rnacomposer.cs.put.poznan.pl/Home/ComposeBatch).

2.11. Statistical analysis

Experiments were conducted in at least three independent experiments each with a minimum of three replicates. Statistical analyis was performed using R software (R core Team, 2023) employing different statistical tests (Kruskal Wallis test with Dunn's correction, 2-way ANOVA, Mann-Whitney test for rank comparison). Only p-values < 0.05 were considered statistically significant.

3. Results

3.1. Clinical history and genetic analysis

The clinical history of the proband and his sister (10 and 7 years old at the last follow up), who presented with symptoms suggestive of a mitochondrial disorder (III-1, III-2) (Fig. 1A) is reported in Supplementary material 1, together with the clinical information of their family members (I-2, II-2, II-3 and II-4). A summary of clinical findings, age at last follow-up, and the HPO used in the genetic analyses are shown in Table 1.

WGS analysis, performed on the proband (III-1) and his parents, both of whom were considered unaffected, identified homoplasmic m.8357T

> C variant in the *MT-TK* gene, which encodes for mt-tRNA-Lys. The whole mtDNA sequence was repeated by Nextera XT protocols in DNA from proband's muscle (average depth of coverage 1,300X) assigned the patient to haplogroup H7a1 and corroborating the homoplasmic condition of m.8357T > C. Homoplasmy for the m.8357T > C variant was confirmed by targeted PCR fragment evaluated with Nextera XT protocol in muscle of both children.

By NGS the variant was also found to be homoplasmic in blood, urine sediment and fibroblast DNA samples from both siblings, while the mother showed levels of heteroplasmy of approximately 80 % across all tissues, including urine, blood and skin derived fibroblasts. The unaffected grandmother (I-2) and uncle (II-4) displayed medium levels of heteroplasmy, while the affected maternal aunt (II-3) showed very high levels of the variant in blood and urine (96 % and 99 % respectively). The levels of heteroplasmy in the family members in different tissues are summarized in Table 2. Finally, Sanger sequencing was performed in tissues from subjects I-2, II-1, II-2, II-3, II-4, III-1, III-2 (Supplementary Fig. S1).

The m.8357T > C variant had already been identified in three adult family members affected by multiple symmetric lipomatosis −with involvement of neck, trunk, and/or proximal parts of upper and lower limbs- in a heteroplasmic condition with a lower mutational load and associated to haplogroup L2d (López-Gallardo et al., 2020). The proband from this Venezuelan family also exhibited brachycephaly and facial asymmetry, bilateral microlithiasis, hyperuricemia and dermatological manifestations —including hyperkeratosis and desquamative lesions— whose onset was at the age of 9 years. These authors confirmed the mtDNA variant pathogenicity by the use of cybrid cell lines.

The m.8357T > C variant is not reported in ClinVar (Landrum et al., 2014) and, with the exception of the sequence deposited by López-Gallardo et al. (López-Gallardo et al., 2020) in MITOMAP (Lott et al., 2013), it is absent both in MITOMAP and gnomAD and not listed in the Helix database. Moreover, the conservation score is 26.67 %, and the MitoTIP score prediction is 13.429 (Sonney et al., 2017), further supporting its potential pathogenicity.

To rule out a dual molecular diagnosis and/or other relevant genetic nDNA variants that could modulate the effect of the m.8357T > C, WES was performed on the affected siblings and their parents, who were considered unaffected (quad WES), as well as on individuals I-2 and II-4, who was considered unaffected too, and II-3 (Fig. S1A).

The m.8357T > C was classified as variant of unknown significance (VUS) according to ACMG-AMP criteria for mtDNA (PS3_supporting, PS4_supporting, PM2_supporting, PP1_supporting; https://wintervar.wglab.org/evds.php) (McCormick et al., 2020).

However, according to the criteria to categorized mt-tRNA variant suggested by Wong et al. (Wong et al., 2020), the m.8357T > C may be classifiable as pathogenic (PS3, PS4, PS5, PM2, PM8, PM9, PP3, PP4 criteria).

Moreover, the absence of other pathogenic variants in nDNA further supports its potential pathogenicity when homoplasmic or near homoplasmic.

Furthermore, in fibroblasts from III to 1, III-2 and II-2, we found an increment of mtDNA copy number, possibly suggesting a compensatory mechanism (reported in Table 3).

Table 3
The mtDNA copy numbers in fibroblasts. *MT-ND1* and *MT-ND3* genes were used as target and were normalized on the genomic *RPPH* gene. The results are shown as ratio of the copy number in control cells.

	III-1	III-2	II-2
MtDNA copy number			
MT-ND1/RPPH	1.37	1.39	1.28
MT-ND3/RPPH	1.37	1.39	1.28

3.2. Functional characterization of m.8357T > C variant

The variant in the *MT-TK* gene is predicted to disrupt base pairing in the acceptor stem of m.tRNA-Lys, potentially altering its structure and function, as suggested by *in silico* modeling of the tRNA structure. As shown in Fig. 1 (panel D), the superimposed structures of the wild-type and mutant tRNA, reveal a modification of the overall conformation, including the anti-codon loop. This may result in impaired mitochondrial protein translation and a subsequent decrease in the activity of the mitochondrial complexes.

To confirm the pathological effect of the genetic variant, mt-tRNA-Lys tRNA levels were evaluated in immortalized fibroblasts derived from the probands, their mother and a control. The mt-tRNA-Lys levels were decreased in both siblings and their mother when normalized to snRNA *RNU6B* and mt-tRNA-Leu(UUR), the tRNA encoded by *MT-TL1*. The expression of *MT-TL1* gene was comparable to that of the control, confirming that mitochondrial DNA transcription was unaffected. The polycistronic transcription of mtDNA may mitigate the presence of the m.8357T > C variant and not alter the tRNA-Lys synthesis (Fernandez-Vizarra and Zeviani, 2021). Therefore, our data suggest that reduction of mtRNA-Lys level might rely on post-transcriptional mechanisms such as reduced stability or increased degradation (Fig. 2).

Then to assess the functional impact of mt-tRNA-Lys reduction, the level of three mitochondrial DNA encoded protein were evaluated. WB analysis showed that the relative expression (normalized on actin) of cytochrome *b* (encoded by *MT-CYB* part of cIII), cytochrome *c* oxidase 1 (encoded by *MT-CO1*, part of cI), and NADH dehydrogenase subunit 1 (encoded by *MT-ND1*, part of cIV), were reduced in the siblings, while only cytochrome *c* oxidase 1 showed a significant decrease in the mother (Fig. 3).

The isolated reduction of mitochondrial cI activity was observed in the muscle samples from both siblings: 34 % and 27 % of the average value of the controls respectively in III-1 and III-2, while the activities of the other complexes resulted normal (Table 4).

To further confirm the mitochondrial impact of the m.8357T > C variant, the enzymatic activities of cI, cIII and cIV were also measured in the immortalized fibroblasts, where a decrease was detected in cI, cIII and cIV activities with cIV being the most affected. In contrast, the fibroblasts from the mother (II-2) did not show any enzymatic activity reduction (Fig. 4).

Secondly, oxygen consumption was measured using high resolution respirometry. Mitochondrial respiration was reduced in all three family members (III-1, III-2 and II-2), with a marked decrease in ETC capacity, following the addition of the mitochondrial uncoupler CCCP, confirming reduced ETC activity particularly under conditions of maximal enzymatic activity stimulation (Fig. 5).

Lastly, we assessed mitochondrial membrane potential (MMP) as a key indicator of mitochondrial function using the JC1 probe, a lipophilic cationic dye that accumulates within mitochondria in a membrane-potential dependent manner, shifting its emission from green to red wavelengths. Under basal condition, MMP did not differ between the probands and control cells. However, in the presence of the mitochondrial OXPHOS uncoupler, CCCP, a significant decrease in MMP was observed. At higher concentration (10 μM) of CCCP, depolarization was similar between control cells and probands. In contrast, when a lower concentration (5 μM) was applied, depolarization was significantly greater in the two siblings and their mother, indicating mitochondrial dysfunction (Fig. 6).

4. Discussion

This study aimed to functionally characterize the m.8357T > C variant, in *MT-TK* gene (encoding for m.tRNA-Lys), identified as homoplasmic in blood in a pediatric male proband and his younger sister, currently 10 and 7 years old respectively. Both of whom exhibited symptoms suggestive for a mitochondrial disorder, including renal

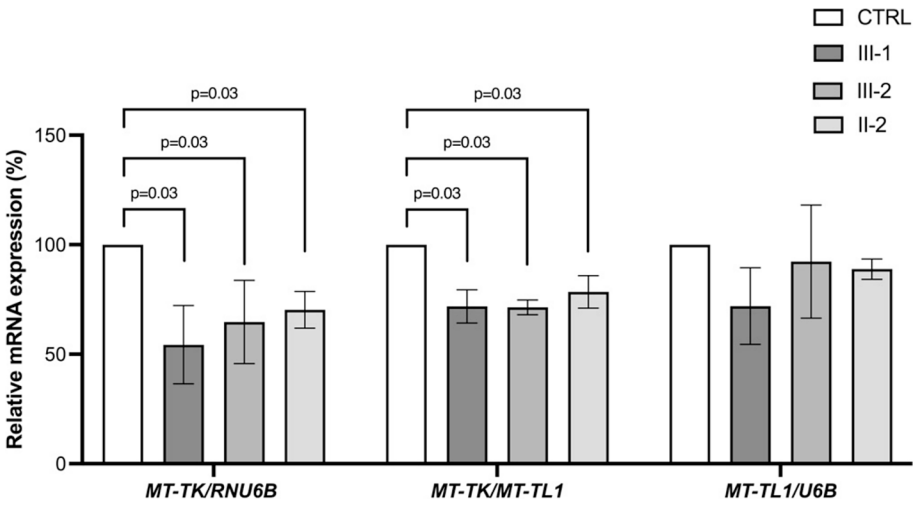

Fig. 2. MT-TK gene expression in the fibroblast cells derived from the two siblings (III-1, III-2) and the mother (II-2). MT-TK tRNA expression was normalized with expression of RNU6B, and MT-TL1 genes. The results are showed as percentage of the relative mRNA expression. Cells from a healthy control (CTRL) were used for normalization. The Mann-Whitney test (comparing ranks) results were also reported. Experiments were conducted four times.

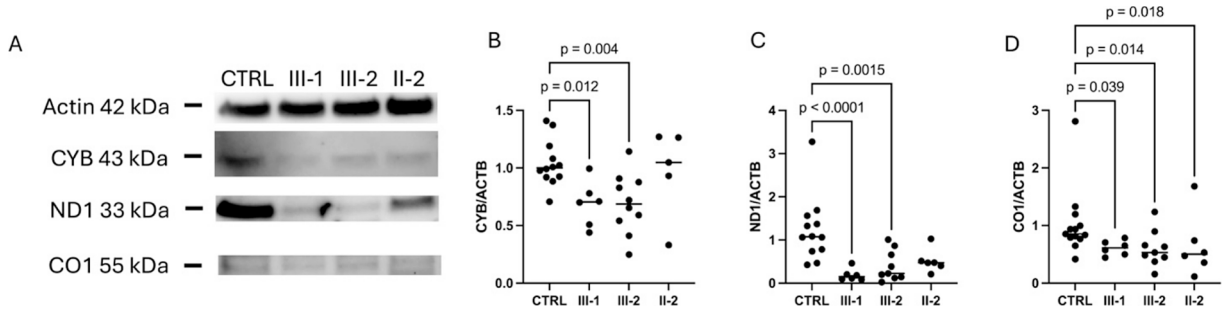

Fig. 3. Western blot analysis of cytochrome *b* (CYB), cytochrome *c* oxidase 1 (CO1) and NADH dehydrogenase subunit 1 (ND1) in the fibroblasts derived from the two siblings (III-1, III-2) and the mother (II-2). The protein density bands are displayed in panel A, while the ratio between the proteins of interest and actin (ACTB) were displayed in panel B (CYB/ACTB), panel C (ND1/ACTB) and panel D (CO1/ACTB). The Kruskal Wallis statistical results were also reported. CTRL control cell lines. Each dot in panel B, C, D represented a replicate. Each experiment was performed in at least four independent replicates.

Table 4
Biochemical activities of mitochondrial complexes performed on muscle samples of the two siblings (III-1 and III-2). The activities were expressed as nmol min-1 mg-1 of protein and normalized for citrate synthase (CS) activity. The control values were indicated as mean ± s.d.

	III-1	III-2	control values
complex I	**8.7**	**6.9**	25.5 ± 4.3
complex II	18.5	15.8	25 ± 5.1
complex III	164	185	150 ± 25.5
complex IV	138	176	135 ± 23.0
SDH	11.5	12.0	11 ± 2.0
CS	162	157	135 ± 33.2

dysfunction with normal anion gap, metabolic acidosis and hyperkalemia, lactic acidosis, epilepsy/abnormalities on electroencephalogram (EEG), hearing loss, fatigability, weakness. Muscle biopsy analysis revealed the homoplasmy of the m.8357T > C variant, associated with decreased activity of mitochondrial cI in this tissue.

Furthermore, the family history was contributory for the maternal aunt, who was affected by intellectual disability. We therefore genotyped the affected siblings' mother and all maternal relatives, including the aunt, for the m.8357T > C variant. High levels of heteroplasmy for the variant in the mother (approximately 80 %) and in the maternal aunt (95–99 %) were detected, while a moderate level of heteroplasmy was found in the healthy maternal grandmother and uncle.

Detection of the mtDNA variant in blood from all family members at different levels of heteroplasmy prompted us to follow a reverse phenotype approach. As a result, we found that the siblings' mother and maternal aunt were affected by mild hearing loss, and that the latter also exhibited easy fatigability and weakness, whereas the uncle and the grandmother were clinically unremarkable.

The sharing of hearing impairment, intellectual disability/developmental delay, and exercise-induced muscle fatigue among the three affected family members (III-1, III-2 and II-3), together with detection of homoplastic levels of the mtDNA variant in their blood, and the presence of hearing impairment in their linking relative II-2 suggested that the variant segregated with the phenotype in the family, and that disease severity correlated with heteroplasmy levels.

To further investigate the role of the variant and its potential pathogenicity, multiple approaches were used, integrating quantitative genetic analyses extended to multiple tissues together with molecular, biochemical and physiological data.

Genetic analysis confirmed the homoplasmic level of m.8357T > C variant in urine and fibroblasts from the siblings and the homoplasmic status remained also unchanged after fibroblast immortalization. The homoplasmy observed in all analyzed tissues suggests the possibility of global homoplasmy, which may explain the multisystem involvement of their disease.

The study of the mtDNA copy number in the fibroblasts from both siblings showed a slight increase of mtDNA copies, possibly indicating a compensatory effect (Filograna et al., 2019).

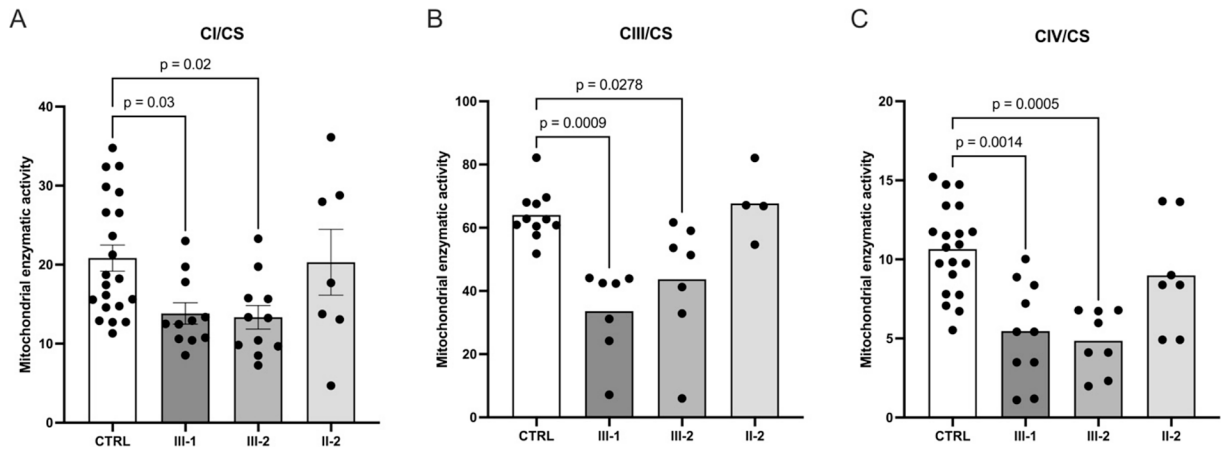

Fig. 4. Enzymatic activity of complex I (cI, panel A), III, (cIII, panel B), and IV (cIV, panel C), normalized on protein content and on citrate synthase (CS) activity in the 2 siblings (III-1, III-2) and in the mother (II-2). The Kruskal Wallis statistical results were also reported. CTRL control cell lines. Each dot in panel represented a replicate. Each experiment was performed in at least four independent assays.

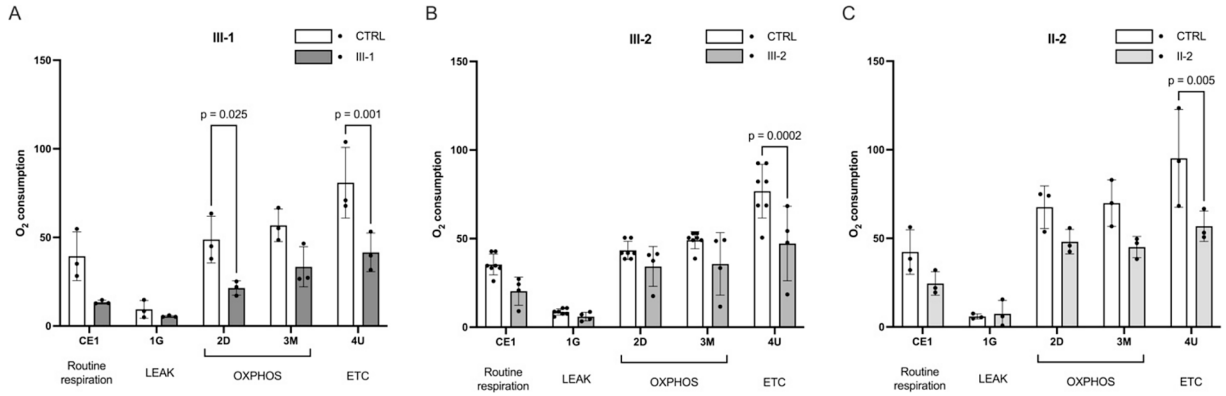

Fig. 5. O_2 consumption measure with high resolution respirometry in the sibling (III-1 and III-2) and the mother (II-2). The white plot indicated the control cell line (CTRL), the light gray the subjects III-1 (panel A), III-2 (panel B), and II-2 (panel C). The 2-way ANOVA statistical results were also reported. Each dot in panel represented a replicate. Each experiment was performed in at least three independent assays.

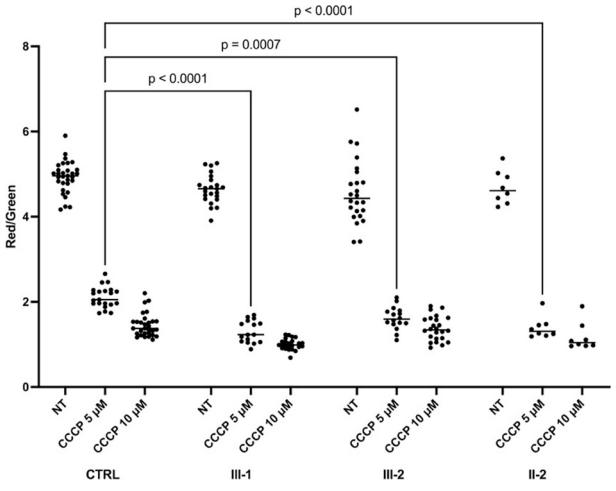

Fig. 6. Mitochondrial membrane potential(MMP) assessed with JC1 probe, the red to green ration are reported in the control cell line (CTRL) in the siblings (III-1 and III-2) and the mother (II-2). The Kruskal Wallis statistical results were also reported ***p < 0.001, **p < 0.01, *p < 0.05. Each dot in panel represented a replicate. Each experiment was performed in at least four independent assays.

Interestingly, the m.8357T > C variant is localized in the acceptor stem of the m.tRNA-Lys, disrupting base pairing and altering the tRNA structure as predicted by *in silico* modelling. The absence of one tRNA component cannot be compensated by a cytoplasmic tRNA, albeit the cytoplasmatic tRNA-Lys is identical to mt.tRNA-Lys, because the inner mitochondrial membrane is impermeable to nucleic acid import (Fernandez-Vizarra and Zeviani, 2021). Therefore this variant may impair the tRNA function in mitochondrial protein translation (Fernandez-Vizarra and Zeviani, 2021).

The mt-tRNA-Lys amount was reduced in the affected siblings, even when normalized to another mitochondrial tRNA, mt-tRNA-Leu(UUR), suggesting that the transcription of the polycistronic mtDNA was unaffected by the variant, as expected. Based on these data it was possible to hypothesize that the mutant tRNA might be less stable and possibly more prone to degradation. Indeed, the protein levels of cytochrome *b*, cytochrome *c* oxidase 1 and NADH dehydrogenase subunit 1, all encoded by mtDNA, were decreased in the two sibs, while only cytochrome *c* oxidase 1 showed a statistically significant decrease in the mother, suggesting a reduced decodifying efficiency of the mutated mt.tRNA-Lys in mitochondrial translation machinery.

Given the reduced protein levels of ETC components, a decrease in the enzyme activity of the associated complexes was predictable.

Indeed, muscle samples from both children showed a significant reduction of cI activity. In fibroblasts, the activities of cI, cIII and cIV were also affected, although less severely than in muscle. These data were confirmed by the decrement of oxygen consumption by high

resolution respirometry, especially the ETC maximal capacity. In this highly sensitive assay, cells from the mother were also affected, even though normal activity levels of cI, cIII and cIV was observed. Finally, fibroblasts derived from the siblings compared to control cells showed higher depolarization of MMP, so that patients' cells were unable to compensate for the depolarizing effect of CCCP to the same level as the control cells.

Altogether our results suggest that the m.8357T > C variant on mt-tRNA-Lys can impair mitoribosome translation subsequently affecting respiratory chain activity, with this effect being more pronounced in the homoplasmic status observed in the two siblings.

In our study, although the mother carried the mitochondrial variant in a heteroplasmic condition and her fibroblasts displayed some *in vitro* evidence of mitochondrial dysfunction, she only experienced mild clinical symptoms, specifically a mild sensorineural hearing loss. In contrast, her children, who were homoplasmic for the same variant, exhibited more severe clinical features, and their maternal aunt also showed clinical symptoms. Of note, WES and WGS failed to discover additional genetic hit(s) explaining the severity of the disease. Therefore, full phenotypic expression of the disease appeared to be associated only with a virtually near-homoplasmic or fully homoplasmic state of this specific mitochondrial DNA variant, whereas heteroplasmy as high as 80 % were associated with a paucisymptomatic presentation (isolated hearing loss).

It has been reported that some mtDNA pathogenic variants may cause disease only at very high mutation loads or in homoplasmic conditions and the same mtDNA pathogenic variant can result in a range of clinical symptoms, influenced, at least in part, by the heteroplasmy levels in the affected tissues or organs and/or interactions with other molecular factors (Rahman, 2020).

The genetic diagnosis of the two siblings was initially uncertain, as this variant was classified as VUS by ACMG-AMP criteria, and it had been previously reported in three adult family members (maternal lineage) exhibiting a completely different phenotype (multiple symmetric lipomatosis) and relative low levels of heteroplasmy in blood (38 %, 43 % and 53–65 %) (López-Gallardo et al., 2020), substantially lower than those found in the two siblings in our study. Moreover, the authors generated homoplasmic cybrids, and observed a reduction of complex IV activity, impaired mitochondrial respiration, low *MT-CO1* encoded protein amount, and defective growth in galactose supplemented medium. These findings closely parallel those observed in our study. Furthermore, the identification of the variant m.8357T > C in different haplogroups (H7a1 for our family, L2d for the Venezuelan family) suggests the pathogenic role of the variant by itself.

In conclusion, our study supports the potential reclassification of the m.8357T > C variant as pathogenic, in accordance with the mt-tRNA variant classification criteria proposed by Wong et al. (Wong et al., 2020).

In this study, it was necessary to complement the genomic analysis on blood and quantitative mtDNA genetic analysis in different tissues with a multidisciplinary clinical and instrumental evaluation. This included deep phenotyping, analysis of blood and urine biomarkers, assessment of metabolic acidosis, biochemical analysis of oxidative phosphorylation and functional *in vitro* characterization of the variant. This integrated approach facilitated a comprehensive characterization of the phenotype associated with the m.8357T > C mtDNA variant, elucidated its pathogenic potential, its role in disease severity, and enabled the definition of the recurrence risk within the family.

Ethical statement

The study was reviewed and approved by the Ethical Committee of the IRCCS Burlo Garofolo (Institutional Review Board, approval number IRB-BURLO 03/2024, 11.04.2024) in accordance with the Declaration of Helsinki.

Author contribution

LZ, MZ conceived the study, LZ designed the experiments. VC, LZ, performed the experiments and analyzed the data. SC and MS performed the *in silico* modelling. G.Girotto and MTB interpreted WES and genetic data. EL and AM performed the genetic and biochemical analysis on the muscle sample. IB, G. Gortani, MTB, and BS evaluated the patients and collected clinical data. LZ wrote the manuscript, MTB wrote the genetic and clinical report paragraphs. All authors revised critically the paper and approved the final version.

CRediT authorship contribution statement

Luisa Zupin: Writing – original draft, Project administration, Methodology, Investigation, Formal analysis, Conceptualization. **Valeria Capaci:** Writing – review & editing, Methodology, Investigation, Formal analysis. **Maria Teresa Bonati:** Writing – original draft, Investigation, Formal analysis, Data curation. **Eleonora Lamantea:** Writing – review & editing, Formal analysis. **Muhammad Suleman:** Writing – review & editing, Formal analysis. **Andrea Marsala:** Writing – review & editing, Formal analysis. **Fulvio Celsi:** Writing – review & editing, Investigation. **Beatrice Spedicati:** Writing – review & editing, Data curation. **Sergio Crovella:** Writing – review & editing, Formal analysis. **Giulia Gortani:** Writing – review & editing, Investigation, Data curation. **Giorgia Girotto:** Writing – review & editing, Investigation, Data curation. **Irene Bruno:** Writing – review & editing, Investigation, Data curation, Conceptualization. **Massimo Zeviani:** Writing – review & editing, Visualization, Supervision, Project administration, Data curation, Conceptualization.

Declaration of competing interest

The authors declare that they have no known competing financial interests or personal relationships that could have appeared to influence the work reported in this paper.

Acknowledgments

This work was supported by the Italian Ministry of Health, through the contribution given to the Institute for Maternal and Child Health IRCCS Burlo Garofolo, Trieste – Italy (grant number RC 10/24; RC 13/24; M-mito, 5M19_5). Biochemical and molecular analyses in muscle biopsy of two children were carried out at the Center for the Study of Mitochondrial Pediatric Diseases funded by the Mariani Foundation in Milan.

Appendix A. Supplementary data

Supplementary data to this article can be found online at https://doi.org/10.1016/j.mito.2025.102080.

References

Abbott, J.A., Francklyn, C.S., Robey-Bond, S.M., 2014. Transfer RNA and human disease. Front. Genet. 5, 158. https://doi.org/10.3389/fgene.2014.00158.

Adzhubei, I., Jordan, D.M., Sunyaev, S.R., 2013. Predicting functional effect of human missense mutations using PolyPhen-2. Current Protocols in Human Genetics Chapter 7 Unit7.20. https://doi.org/10.1002/0471142905.hg0720s76.

Bergonzini, L., Carli, S., Pelle, S., Pettenuzzo, I., Bonetti, S., Santi, E., Visconti, C., Maffei, M., Sheremet, M., Lamantea, E., Marsala, A., Klub, O., Gentile, V., Cordelli, D.M., Garone, C., 2025. Infantile TK2 deficiency causing mitochondrial encephalomyopathy with migrating focal seizures. Neurology 104, e213373. https://doi.org/10.1212/WNL.0000000000213373.

Bugiani, M., Invernizzi, F., Alberio, S., Briem, E., Lamantea, E., Carrara, F., Moroni, I., Farina, L., Spada, M., Donati, M.A., Uziel, G., Zeviani, M., 2004. Clinical and molecular findings in children with complex I deficiency. BBA 1659, 136–147. https://doi.org/10.1016/j.bbabio.2004.09.006.

El-Hattab, A.W., Adesina, A.M., Jones, J., Scaglia, F., 2015. MELAS syndrome: Clinical manifestations, pathogenesis, and treatment options. Mol. Genet. Metab. 116, 4–12. https://doi.org/10.1016/j.ymgme.2015.06.004.

Fernandez-Vizarra, E., Zeviani, M., 2021. Mitochondrial disorders of the OXPHOS system. FEBS Lett. 595, 1062–1106. https://doi.org/10.1002/1873-3468.13995.
Filograna, R., Koolmeister, C., Upadhyay, M., Pajak, A., Clemente, P., Wibom, R., Simard, M.L., Wredenberg, A., Freyer, C., Stewart, J.B., Larsson, N.G., 2019. Modulation of mtDNA copy number ameliorates the pathological consequences of a heteroplasmic mtDNA mutation in the mouse. Sci. Adv. 5, eaav9824. https://doi.org/10.1126/sciadv.aav9824.
Grazina, M.M., 2012. Mitochondrial respiratory chain: biochemical analysis and criterion for deficiency in diagnosis. Methods in molecular biology (Clifton N.J.) 837, 73–91. https://doi.org/10.1007/978-1-61779-504-6_6.
Jacobs, H.T., 2003. Disorders of mitochondrial protein synthesis. Hum. Mol. Genet. 12, R293–R301. https://doi.org/10.1093/hmg/ddg285.
Landrum, M.J., Lee, J.M., Riley, G.R., Jang, W., Rubinstein, W.S., Church, D.M., Maglott, D.R., 2014. ClinVar: public archive of relationships among sequence variation and human phenotype. Nucl. Acids Res. 42, D980–D985. https://doi.org/10.1093/nar/gkt1113.
Legati, A., Zanetti, N., Nasca, A., Peron, C., Lamperti, C., Lamantea, E., Ghezzi, D., 2021. Current and new next-generation sequencing approaches to study mitochondrial DNA. J. Mol. Diagn. 23, 732–741. https://doi.org/10.1016/j.jmoldx.2021.03.002.
López-Gallardo, E., Cammarata-Scalisi, F., Emperador, S., Hernández-Ainsa, C., Habbane, M., Vela-Sebastián, A., Bayona-Bafaluy, M.P., Montoya, J., Ruiz-Pesini, E., 2020. Mitochondrial DNA pathogenic mutations in multiple symmetric lipomatosis. Clin. Genet. 97, 731–735. https://doi.org/10.1111/cge.13701.
Lott, M.T., Leipzig, J.N., Derbeneva, O., Xie, H.M., Chalkia, D., Sarmady, M., Procaccio, V., Wallace, D.C., 2013. mtDNA variation and analysis using mitomap and mitomaster. Curr. Protoc. Bioinformatics 44, 1.23.1-26. https://doi.org/10.1002/0471250953.bi0123s44.
McCormick, E.M., Lott, M.T., Dulik, M.C., Shen, L., Attimonelli, M., Vitale, O., Karaa, A., Bai, R., Pineda-Alvarez, D.E., Singh, L.N., Stanley, C.M., Wong, S., Bhardwaj, A., Merkurjev, D., Mao, R., Sondheimer, N., Zhang, S., Procaccio, V., Wallace, D.C., Gai, X., Falk, M.J., 2020. Specifications of the ACMG/AMP standards and guidelines for mitochondrial DNA variant interpretation. Hum. Mutat. 41, 2028–2057. https://doi.org/10.1002/humu.24107.
Ojala, D., Montoya, J., Attardi, G., 1981. tRNA punctuation model of RNA processing in human mitochondria. Nature 290, 470–474. https://doi.org/10.1038/290470a0.
R core Team, 2023. R: a Language and Environment for Statistical Computing.
Rahman, S., 2020. Mitochondrial disease in children. J. Intern. Med. 287, 609–633. https://doi.org/10.1111/joim.13054.
Richards, S., Aziz, N., Bale, S., Bick, D., Das, S., Gastier-Foster, J., Grody, W.W., Hegde, M., Lyon, E., Spector, E., Voelkerding, K., Rehm, H.L., 2015. Standards and guidelines for the interpretation of sequence variants: a joint consensus recommendation of the American college of medical genetics and genomics and the association for molecular pathology. Genet. Med. 17, 405–424. https://doi.org/10.1038/gim.2015.30.
Richter, U., McFarland, R., Taylor, R.W., Pickett, S.J., 2021. The molecular pathology of pathogenic mitochondrial tRNA variants. FEBS Lett. 595, 1003–1024. https://doi.org/10.1002/1873-3468.14049.
Sonney, S., Leipzig, J., Lott, M.T., Zhang, S., Procaccio, V., Wallace, D.C., Sondheimer, N., 2017. Predicting the pathogenicity of novel variants in mitochondrial tRNA with MitoTIP. PLoS Comput. Biol. 13, e1005867. https://doi.org/10.1371/journal.pcbi.1005867.
Suzuki, T., Yashiro, Y., Kikuchi, I., Ishigami, Y., Saito, H., Matsuzawa, I., Okada, S., Mito, M., Iwasaki, S., Ma, D., Zhao, X., Asano, K., Lin, H., Kirino, Y., Sakaguchi, Y., Suzuki, T., 2020. Complete chemical structures of human mitochondrial tRNAs. Nat. Commun. 11, 4269. https://doi.org/10.1038/s41467-020-18068-6.
Suzuki, T., Nagao, A., Suzuki, T., 2011. Human mitochondrial tRNAs: biogenesis, function, structural aspects, and diseases. Annu. Rev. Genet. 45, 299–329. https://doi.org/10.1146/annurev-genet-110410-132531.
Velez-Bartolomei, F., Lee, C., Enns, G., 1993. MERRF. In: Adam, M.P., Feldman, J., Mirzaa, G.M., Pagon, R.A., Wallace, S.E., Bean, L.J., Gripp, K.W., Amemiya, A. (Eds.), GeneReviews®. University of Washington, Seattle, Seattle (WA).
Wong, L.-J.-C., Chen, T., Wang, J., Tang, S., Schmitt, E.S., Landsverk, M., Li, F., Wang, Y., Zhang, S., Zhang, V.W., Craigen, W.J., 2020. Interpretation of mitochondrial tRNA variants. Genet. Med. 22, 917–926. https://doi.org/10.1038/s41436-019-0746-0.